*Clays and Clay Minerals*, Vol. 34, No. 2, 214–223, 1986.

# IDEALITY OF CLAY MEMBRANES IN OSMOTIC PROCESSES: A REVIEW

STEVEN J. FRITZ

Department of Geology, Texas A&M University
College Station, Texas 77843

**Abstract**—Clays can act as osmotic membranes and thus give rise to osmotically induced hydrostatic pressures. The magnitude of generated osmotic pressures in geologic systems is governed by the theoretical osmotic pressure calculated solely from solution properties and by value of the membrane's three phenomenological coefficients: the hydraulic permeability coefficient, $L_p$; the reflection coefficient, $\sigma$; and the solute permeability coefficient, $\omega$. Generally, low values of $L_p$ correspond to highly compacted membranes in which $\sigma$ is near unity and $\omega$ approaches zero. Such membrane systems should give rise to initially high osmotic fluxes and gradual dissipation of their osmotic potentials.

The high fluid pressures in the Dunbarton Triassic basin, South Carolina, are a good example of osmotically induced potentials. A unique osmotic cell is created by the juxtaposition of fresh water in the overlying Cretaceous sediments against the saline pore water housed within the membrane-functioning sediments of the Triassic basin. Because wells penetrating the saline core of the basin show anomalously high heads relative to wells penetrating the basin margins, the longevity of this osmotic cell is probably dictated by the rate at which salt diffuses out into the overlying fresh water aquifer.

**Key Words**—Clay osmosis, Hydraulic permeability, Hydraulic pressure, Membrane, Osmotic pressure, Solute permeability.

## INTRODUCTION

Experimental studies have shown that clay membranes give rise to electroosmosis (Hanshaw, 1962; Srivastava and Avasthi, 1975), hyperfiltration (McKelvey and Milne, 1962; Kharaka and Smalley, 1976), and regular (chemical) osmosis (Young and Low, 1965; Kemper and Rollins, 1966; Olsen, 1969). Osmosis through clays has been invoked to explain such disparate phenomena in the subsurface as anomalous hydraulic heads (Marine, 1974), thrust faulting (Hanshaw and Zen, 1965), and breaching of clay liners of seepage ponds holding saline waste (Hudec, 1980). The membrane behavior of particular interest to petroleum geologists is the generation of osmotic pressure in the subsurface. Osmosis may be important in oil fields where clays and shales commonly separate waters of different salinity. In these situations, osmosis, and not the presence of gaseous hydrocarbons, may cause anomalously high fluid pressures (Marine, 1974).

Porous media behave as osmotic membranes if they have salt-rejecting capabilities. It is the degree of ideality of geologic membranes that largely controls the magnitude of osmotically induced hydrostatic pressure in the subsurface. The objective of the present paper is to review the physiochemical factors affecting the degree of ideality of clay membranes as they relate to the generation and dissipation of osmotic pressures in the subsurface. Because many earth scientists are only slightly familiar with the workings of osmosis, this paper also reviews the principles of this geologically important phenomenon.

## SALT-EXCLUSIONARY PROPERTIES OF CLAY MEMBRANES

A membrane is a semi-permeable barrier which permits the transport of some components of a solution and not others (Tuwiner, 1962). A membrane rejects solutes on the basis of size and/or electrical restrictions (Gregor and Gregor, 1978). Geologic membranes have pore sizes generally large enough to accommodate the largest hydrated radii of ions commonly found in ground water. Thus, the salt-exclusionary behavior of clay membranes is due to electrical restrictions operating within the interstices of clay membrane structures.

The surfaces of clay minerals have a net negative charge (White, 1965) which is mainly a result of substitution of lower-valence cations for higher-valence cations within the structure (Grim, 1968). This charge deficiency is manifested at the surface of the platelets where neutralization takes place by sorption of cations in the vicinity of the negatively charged substrate. The charged surface of the clay and its cation-dominated sorption layer together define the Guoy double layer (Stumm and Morgan, 1970).

The salt-exclusionary properties of clays arise when compaction of a clay slurry induces overlap of double layers of adjacent platelets. This overlap results in the pore space between clay platelets having a negative electrical potential. Anions attempting to migrate through such pores are thus repelled as are cations because the cations must remain with their anionic counterparts to retain electrical neutrality in the outer, or "free" solution. Water, of course, is freely admitted to the membrane structure.

The pores of ideal membranes contain no free salt, i.e., solutes are not bound in the cation-dominated sorption layer. Non-ideal membranes, however, contain solute within their pores. The concentration of salt within such negatively charged membranes, $\bar{C}_a$, is defined on the basis of the normality of anions within pores unaffected by the double layer (Katchalsky and Curran, 1965). The value of $\bar{C}_a$ can be calculated by the Teorell-Meyer-Siever Model as expressed by Hanshaw (1962):

$$\bar{C}_a = -\tfrac{1}{2}E\cdot\rho\cdot(1 - \phi_w) + \tfrac{1}{2}[E^2\cdot\rho^2\cdot(1 - \phi_w)^2 + 4\bar{c}_s^2\phi_w^2]^{1/2}. \quad (1)$$

Thus, the degree of salt exclusion of a clay membrane is a function of the cation-exchange capacity (CEC) of the clay (E, in equiv/g), dry density ($\rho$, in g/cm$^3$), the porosity of the membrane ($\phi_w$), and mean concentration of salt for the solution on either side of the membrane ($\bar{c}_s$, in equiv/cm$^3$).

All clays are non-ideal membranes, but the efficacy of their salt exclusion is greatest when a high-CEC clay of low porosity separates dilute solutions (Marine and Fritz, 1981). Greater overlap of double layers promotes more efficient exclusion of salt by the membrane structure. Eq. (1) shows that as the porosity tends toward zero, $\bar{C}_a$ approaches zero. For two clay membranes of identical porosity, the clay with the higher surface-charge density will be more ideal. Thus, smectite membranes are inherently more ideal than kaolinite membranes. Eq. (1) also shows that if $\bar{c}_s$ is very small, $\bar{C}_a$ approaches zero; however, the ion-exclusionary property of the double layers can be rendered ineffective if these pores are inundated with salt from an environment outside the membrane structure. If $\bar{c}_s$ is very large, Eq. (1) shows that $\bar{C}_a$ approaches $\bar{c}_s\phi_w$. For non-permselective porous media, $\bar{C}_a = \bar{c}_s$, whereas $\bar{C}_a$ is zero for ideal membranes.

## OSMOSIS IN IDEAL AND NON-IDEAL MEMBRANE SYSTEMS

### *Ideal membranes*

If a membrane separates reservoirs containing solutions of unequal salt concentrations, the difference of the activity of water in the solutions on either side of the membrane drives water through the membrane to the reservoir containing the more saline solution. This process is osmosis. If the membrane is ideal, the passage of salt is totally barred such that only water is transported through the membrane. If the membrane is non-ideal, salt also diffuses through the membrane, but in a direction opposite to that of the osmotically driven flux of water.

The driving force for osmosis is the difference in chemical potential of the water in the two solutions on either side of the membrane ($\Delta\mu_w$). In an isothermal system, the difference of chemical potential of water across the membrane between solution II and solution I is:

$$\Delta\mu_w = \mu_w^{II} - \mu_w^{i} = \bar{V}_w\Delta P - \bar{V}_w\Delta\Pi, \quad (2)$$

where $\bar{V}_w$ is the mean partial molar volume of the water on either side of the membrane in liter/mole; $\Delta P$ is the hydrostatic pressure difference across the membrane in dyne/cm$^2$; and $\Delta\Pi$ is the theoretical osmotic pressure existing across the membrane in dyne/cm$^2$. The theoretical osmotic pressure is a function of the difference of activities of water in the two solutions ($a_w^{II}$ and $a_w^{I}$) across the membrane:

$$\Delta\Pi = (RT/\bar{V}_w)\cdot\ln(a_w^{I}/a_w^{II}), \quad (3)$$

where R = 0.08205 liter·atm/mole·°K and T is temperature in °K. An approximate calculation for $\Delta\Pi$ is given by:

$$\Delta\Pi \sim \nu RT\Delta C = \nu RT(C_{II} - C_I), \quad (4)$$

where $\nu$ is the number of constituent ions of the dissociating solute and $\Delta C$ is the difference of solute concentration of the solutions expressed in terms of molarity. For 1:1 electrolytes like NaCl, $\Delta\Pi$ calculated from Eq. (4) is within 5% of that calculated from Eq. (3), if $\Delta C$ in Eq. (4) is less than 1 M.

For ideal membranes, the observed osmotic pressure equals that predicted by Eq. (3). Here, the observed osmotic pressure is solely a function of the physiochemical properties of the solution affecting the activity of water in that solution. The activity of water is proportional to the molality of the solute (m) and the molal weight of water (M), as well as $\nu$. The activity of water can easily be measured by an osmometer; however, in the absence of a direct measurement, the activity of water can be computed by:

$$a_w = \exp(-\Phi\nu mM), \quad (5)$$

where the proportionally constant, $\Phi$, is the osmotic coefficient. The value of $\Phi$ is unique for any particular solute and is temperature dependent (Robinson and Stokes, 1959). Thus, equal molalities of different salt solutions do not yield the same osmotic pressures because each salt has a unique osmotic coefficient. Salts dissociating into more than two ions depress the activity of water more than salts dissociating into two ions. Inasmuch as lower activities of water translate to higher osmotic potentials, then equimolal solutions of $Na_2SO_4$ and $CaCl_2$ ($\nu = 3$) give higher theoretical osmotic pressures than equimolal solutions of NaCl and $CaSO_4$ ($\nu = 2$).

### *Non-ideal membranes*

In an ideal membrane, the predicted (theoretical) osmotic pressure equals the observed, osmotically induced hydrostatic pressure ($\Delta P$). In non-ideal membranes, typical of clay membrane systems, the hydro-

static pressure generated by osmosis is less than that predicted by Eq. (3). Staverman (1952) assigned the ratio of observed, osmotically induced hydrostatic pressure to theoretical osmotic pressure as the "reflection coefficient," $\sigma$, where

$$\sigma = (\Delta P/\Delta\Pi)_{J_v=0}. \quad (6)$$

The net flux of solution across the membrane ($J_v$) is subscripted in Eq. (6) to denote that $\sigma$ is defined when $J_v = 0$. The reflection coefficient measures the ideality of an osmotic system. For ideal membrane systems, $\sigma = 1$; for porous media having no membrane properties, $\sigma = 0$. This latter behavior is herein termed "nonpermselective."

The reflection coefficient is but one of three practical phenomenological coefficients that can be used to describe the behavior of non-ideal membrane systems. Using the framework of non-equilibrium thermodynamics, Kedem and Katchalsky (1962) derived two equations relating the flux of solution ($J_v$, in cm/sec) and solute ($J_s$, in mole/cm$^2$·sec) to differences in hydrostatic and osmotic pressures operating across a membrane:

$$J_v = L_p\Delta P - \sigma L_p\Delta\Pi, \text{ and} \quad (7)$$

$$J_s = \bar{c}_s(1 - \sigma)J_v + \omega\Delta\Pi. \quad (8)$$

Kedem and Katchalsky (1962) defined three practical phenomenological coefficients ($\sigma$, $L_p$, and $\omega$) whose values are empirically determined when certain fluxes and forces are experimentally coerced to vanish. The $\bar{c}_s$ term in Eq. (8) is the arithmetic mean of solute concentration across the membrane in terms of mole/cm$^3$.

*Hydraulic permeability coefficient, $L_p$.* The hydraulic permeability coefficient, $L_p$ (having units of cm$^3$/dyne·sec), relates the fluid discharge through the membrane in response to an applied, or developed, pressure difference, $\Delta P$. $L_p$ is related to the conventional permeability coefficient (K, in cm/sec), by dividing K by the fluid density ($\rho$, in g/cm$^3$), gravitational constant (g, in cm/sec$^2$), and thickness of the membrane (x, in cm):

$$L_p = K/\rho gx. \quad (9)$$

Because the hydraulic permeability coefficient is a ratio of $J_v$ to $\Delta P$, its value is measured when no osmotic potential exists across the membrane, i.e., when $\Delta\Pi = 0$.

*The reflection coefficient, $\sigma$.* Of the three practical phenomenological coefficients, the reflection coefficient, $\sigma$, is the most informative because its value determines the maximum expected osmotically induced pressure developed during the evolution of an osmotic cell (Marine and Fritz, 1981). In non-ideal membrane systems so typical of clay membranes where $0 < \sigma < 1$, the hydrostatic pressure generated by osmosis is less than that predicted solely by Eqs. (3) or (4).

Using the premise that at osmotic equilibrium the thermodynamic forces acting across a membrane are counterbalanced by the sum of mechanical frictional forces of salt and water within the membrane, Marine and Fritz (1981) derived an equation for $\sigma$. Their model relates the value of the reflection coefficient to the porosity and surface-charge density of the membrane and to the mean solute concentration on either side of the membrane:

$$\sigma = 1 - \frac{K_s(R_w + 1)}{\{[R_w(\bar{C}_a/\bar{C}_c) + 1] + R_{wm}[R_m(\bar{C}_a/\bar{C}_c) + 1]\}\phi_w}, \quad (10)$$

where $K_s = \bar{C}_a/\bar{c}_s$ and $\bar{C}_c = \bar{C}_a + E\cdot\rho\cdot(1 - \phi_w)$. The distribution coefficient of salt within the membrane pores, $K_s$, is a ratio of the anion concentration within the membrane pores ($\bar{C}_a$) to the mean anion (or solute) concentration outside the membrane, $\bar{c}_s$. The $\bar{C}_a$ term can be calculated by Eq. (1). The $\bar{C}_c$ term is the concentration of cations within the membrane pores.

In Eq. (10), the R terms are ratios of frictional coefficients such that: (1) $R_w$ is the ratio of frictional coefficients of the cation (c) and anion (a) with water (w) in the membrane such that $R_w = f_{cw}/f_{aw}$; (2) $R_{wm}$ is the ratio of frictional coefficients of the cation and anion with the membrane structure; i.e., $f_{cm}/f_{am}$; and (3) $R_{wm}$ is the ratio of frictional coefficients of the anion and solid membrane matrix to the anion and water in the membrane structure. Thus, $R_{wm} = f_{am}/f_{aw}$. The units of individual frictional coefficients, $f_{ij}$, are dyne·sec/cm·mole. The numerical value of $f_{ij}$ represents the frictional resistance of one mole of species i with an infinite amount of species j (Katchalsky and Curran, 1965).

In discussing the values of the R coefficients in the evaluation of $\sigma$ for clay membranes in a NaCl-$H_2O$ system, Marine and Fritz (1981) made several assumptions concerning the behavior of these constants. If the frictional resistance between the cation and the anion in the membrane is equivalent to that in the free solution, the reciprocal of the transport number of the cation in free solution ($1/t^0_{Na^+}$) equals $R_w + 1$. Because the mean value of $t^0_{Na^+}$ in NaCl-$H_2O$ systems is 0.38 and is reasonably independent of concentration (Miller, 1966), $R_w = 1.63$. If the frictional resistance between $Na^+$ and $Cl^-$ in the membrane is independent of electrostatic effects between these two ions, the frictional resistance of these ions with the solid membrane structure should be a purely physical phenomenon. Here, $R_m$ is approximated by the ratio of the hydrated radius of $Na^+$ to the hydrated radius of $Cl^-$, about 1.8 according to Harned and Owen (1958).

As a membrane becomes less porous, the frictional resistance between the anion and the membrane becomes large. Thus, for membranes of very low porosity, $R_{wm}$ becomes significantly larger than 1. Decreasing the porosity also tends to promote overlap of the double layers such that $\bar{C}_a$ becomes very small. Thus, a

https://doi.org/10.1346/CCMN.1986.0340212 Published online by Cambridge University Press

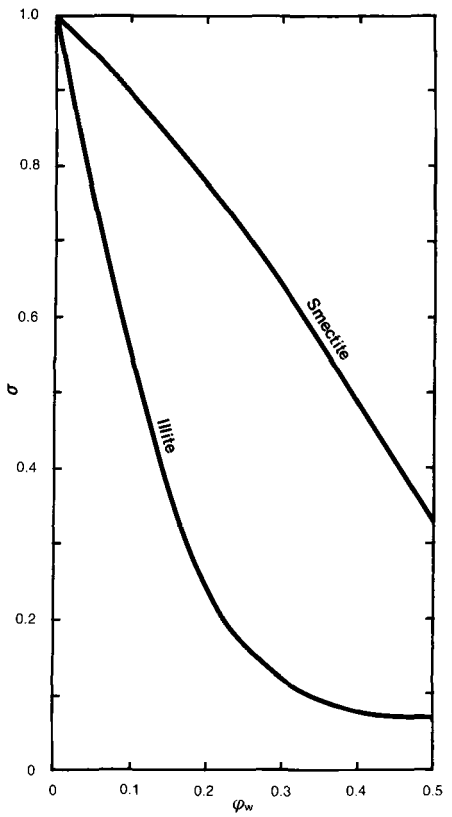


Figure 1. Relationship of reflection coefficient ($\sigma$) to porosity ($\phi_w$) for illite and smectite membranes at fixed $\bar{c}_s$ for NaCl of 0.001 mole/cm³.

reduction of porosity lowers the values for both $K_s$ and $\bar{C}_a/\bar{C}_c$ in Eq. (10). All these effects tend to make $\sigma$ approach unity. In contrast, a highly porous membrane results in little frictional resistance between the anion and the membrane walls. Here, $R_{wm}$ approaches 0. The low degree of double-layer overlap in highly porous membranes also causes $K_s$ and the $\bar{C}_a/\bar{C}_c$ terms to increase toward unity. In this situation, Eq. (10) indicates that $\sigma$ approaches 0. Olsen (1969) verified experimentally this trend for kaolinite membrane in NaCl systems. At a porosity of 59%, the reflection coefficient for the kaolinite membrane was 0.014; whereas, upon compacting the same sample to a porosity of 10%, the value of $\sigma$ was 0.366. This trend was also corroborated by Fritz and Marine (1983) in their experimental studies of Na-bentonites.

Figure 1 shows the variation of $\sigma$ as a function of porosity for two monomineralic clay membranes, an illite having a CEC of 20 meq/100 g and a smectite having a CEC of 100 meq/100 g. Both minerals were assumed to have a dry density of 2.61 g/cm³. By assuming that the average concentration about the membrane is $10^{-3}$ mole/cm³, the $\bar{C}_a$ term can thus be calculated by Eq. (1) as a function of $\phi_w$. Eq. (10) was used to calculate the reflection coefficients of these two membranes. The $R_{wm}$ term in Eq. (10) was assumed to be 0.1 throughout the entire range of the porosities portrayed in Figure 1. As stated above, $R_w$ has an assigned value of 1.63, and $R_m$ is 1.8.

Figure 1 shows the dramatic effect of porosity on the ideality of these membranes expressed as $\sigma$. As the porosity decreases toward 0, anion exclusion becomes so effective that even the low-CEC illite approaches ideality. This illustration also demonstrates the inherently more-ideal character of the smectite membrane. Due to its higher surface-charge density, the smectite $\sigma$ always exceeds that of illite when the ideality of these two membranes is compared at the same porosity. Thus, an inherently inefficient membrane composed of kaolinite can be rendered more ideal by compaction. Alternately, a highly porous smectite could be almost non-permselective.

The concentration of salt outside the membrane also has a profound effect on the ideality of a clay membrane. Figure 2 shows the relation between osmotically induced hydrostatic pressure, $\sigma\Delta\Pi$, and mean molar concentration of NaCl on either side of an illite membrane whose porosity is a constant 0.25. Again, $\sigma$ is calculated by Eq. (10). The three curves depict the realized osmotic pressures at osmotic equilibrium for solutions on either side of the membrane having concentration ratios of 9, 3, and 1.5. Thus, for the top curve, $C_{II}/C_I = 9$. Identical salt concentrations of solutions on either side of the membrane result in a ratio of unity. This situation results in no theoretical osmotic pressure as calculated by Eq. (4). For this reason, the curve denoting the ratio of $C_{II}/C_I = 1.5$ exhibits the lowest generated osmotic pressures. Figure 2 shows that the maximum realized osmotic pressure occurs when a membrane is imbibed in solutions of moderate concentration. At low values of $\bar{c}_s$, the illite membrane is highly ideal. For a $\bar{c}_s$ value of $10^{-5}$ mole/cm³, $\sigma$ = 0.985. Here, the theoretical osmotic pressure as calculated by Eq. (4) is very low which in turn results in low values for $\sigma\Delta\Pi$ in this very dilute system. In contrast, the theoretical osmotic pressure can be very high when a membrane separates solutions having large differences of salt concentration, $\Delta C$; however, in such systems, $\sigma$ becomes very low. For $\bar{c}_s = 0.002$ mole/cm³ (i.e., 2 M), $\sigma = 0.076$. This low value of $\sigma$ translates to a lower value of $\sigma\Delta\Pi$ for the membrane system having higher values of $\bar{c}_s$ than for $\sigma\Delta\Pi$ values calculated for systems having intermediate values of $\bar{c}_s$. Thus, higher osmotically induced pressures are more likely to occur in the subsurface where a clay membrane separates solutions of moderate concentration differences than if a clay membrane separates solutions of large concentration differences.

The Fritz-Marine membrane model was experimentally tested by Fritz and Marine (1983). In that study, reflection coefficients of a Na-bentonite were measured as a function of porosity and $\bar{c}_s$. Six experimental values

https://doi.org/10.1346/CCMN.1986.0340212 Published online by Cambridge University Press

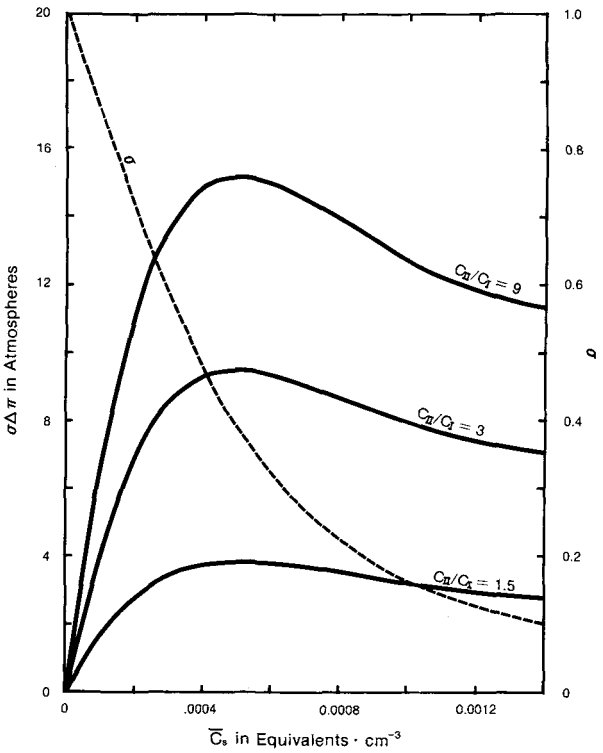


Figure 2. Relationship of osmotically induced hydrostatic pressure ($\sigma\Delta\Pi$) as function of $\bar{c}_s$ for illite membrane having fixed porosity of 0.25. Here, $\bar{c}_s = (C_\Pi + C_l)/2$. $\sigma$ was calculated by Eq. (10); its variation with $\bar{c}_s$ is shown by dashed curve. Three different curves for $\sigma\Delta\Pi$ are drawn to emphasize $\Delta\Pi$ is function of $\Delta C$ such that $\Delta\Pi \cong 2RT(C_\Pi - C_l)$.

of $\sigma$ were all within 0.05 of the values for $\sigma$ computed by Eq. (10). Moreover, the trends depicted in Figure 2 were also corroborated by Fritz and Marine (1983) who reported that osmotically induced back pressure in their hyperfiltration runs was greatest with a 0.1 M NaCl input solution. For input stock solutions of 0.01 and 1.0 M, however, the osmotically induced back pressures were less than the 0.88 MPa back pressure generated in the hyperfiltration of the 0.1 M NaCl solution.

*Solute permeability coefficient, $\omega$.* The solute permeability coefficient, $\omega$ (having units of mole/dyne·sec), is a diffusion coefficient of the solute through the membrane structure. Its value controls the rate at which the saline side of an osmotic cell diffuses its salt across the membrane to the more dilute reservoir. The solute permeability coefficient is defined as the ratio of $J_s$ to $\Delta\Pi$, measured when $J_v = 0$ (Eq. (8)). For ideal membrane systems, $J_s = 0$. As interpreted by Eq. (8), this ideal condition means that salt can neither be transported through the membrane by advection ($\sigma = 1$) nor by diffusion ($\omega = 0$). In non-ideal membranes, $\omega$ takes on positive values and approaches a maximum value ($\omega = [J_s - \bar{c}_s \cdot J_v]/\Delta\Pi$) when $\sigma = 0$.

It should be emphasized that $\omega$ is *not* equivalent to the Fickian diffusion coefficient (D) in free solution because the $\omega$ term incorporates the physical and electrical impedance of the membrane to the diffusive path of an ion through this structure. The value of $\omega$ is a function of the salt-exclusionary property of the membrane ($K_s$), membrane thickness ($\Delta x$), and frictional resistance within the membrane of the anion with the water ($f_{aw}$) and of the anion with the membrane structure ($f_{am}$). Katchalsky and Curran (1965) derived an equation relating these factors to the solute permeability coefficient:

$$\omega = \frac{K_s}{\Delta x \cdot (f_{aw} + f_{am})} . \qquad (11)$$

Because $R_{wm} = f_{am}/f_{aw}$, this equation can be rewritten as:

$$\omega = \frac{K_s}{\Delta x \cdot f_{aw}(1 + R_{wm})} . \qquad (12)$$

If the membrane is ideal ($\sigma = 1$), $\bar{C}_a = 0$. Therefore, $K_s$ ($=\bar{C}_a/\bar{c}_s$) is 0 so that $\omega$ also becomes 0. Alternatively, if the porous medium is non-permselective ($\sigma = 0$), $K_s = 1$. This latter situation is largely brought about by porosity tending toward unity. Thus, as $\phi_w \rightarrow 1$, $R_{wm} \rightarrow 0$, and for a 100% porosity membrane (corresponding to free solution without any solid obstruction), Eq. (12) reduces to

$$\omega = \frac{1}{f^0_{aw} \cdot \Delta x} , \qquad (13)$$

where $f^0_{aw}$ is the frictional coefficient between the anion and the water in free solution. Inasmuch as $f^0_{aw} = RT/D$ (Katchalsky and Curran, 1965), $f^0_{aw}$ for $Cl^-$ in the coupled transport of $Na^+$-$Cl^-$ is about $2.5 \times 10^{15}$ dyne·sec/mole·cm at 298°K. This relation assumes that $D_{NaCl} = 10^{-5}$ cm$^2$/sec and $\Delta x = 1$ cm. If the frictional resistance between the anion and water in free solution is less than that in the pores of a membrane (i.e., $f^0_{aw} < f_{aw}$), Eq. (13) shows that the maximum value of $\omega$ for diffusion of the co-ion through 1 cm will be $4 \times 10^{-16}$ mole/dyne·sec.

As a membrane's porosity is decreased, the efficiency of salt exclusion is increased, resulting in lower values of $K_s$. Decreasing porosity also causes increased frictional resistance between the solute and the membrane structure. Here, the value of $R_{wm}$ increases in Eq. (12). Thus, compaction-induced effects render smaller values of $\omega$ with lower porosities. These combined effects should result in slower diffusion of salts through the membrane structure which retards the rate at which osmotically induced pressure is dissipated.

## OSMOTIC EVOLUTION IN IDEAL AND NON-IDEAL SYSTEMS

The osmotic process is aptly illustrated by a simple U-tube model. Figures 3 and 4 show the evolution of

https://doi.org/10.1346/CCMN.1986.0340212 Published online by Cambridge University Press

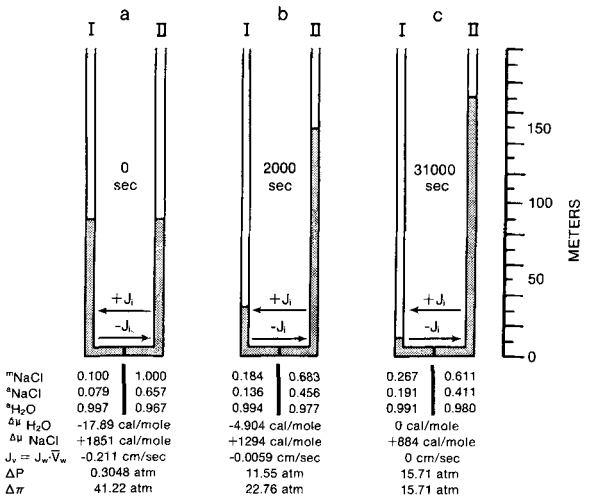


Figure 3. Osmotic evolution in ideal membrane system portrayed by open-ended U-tube models. In this system, osmotic evolution is achieved in 31,000 seconds. Negative fluxes are defined as being left to right.

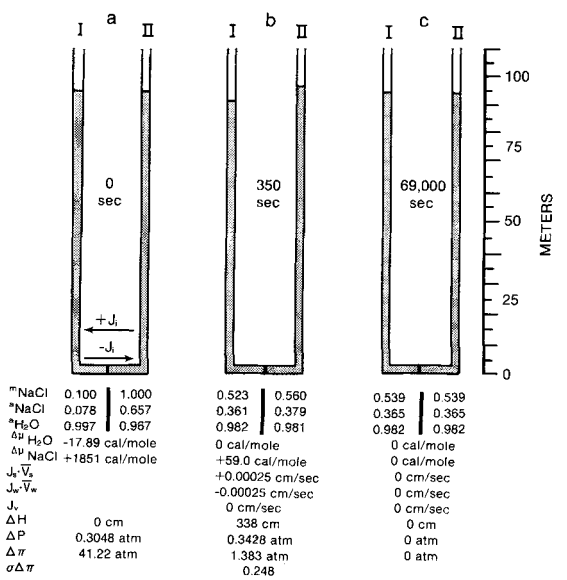


Figure 4. Osmotic evolution in non-ideal membrane system portrayed by open-ended U-tube models. True equilibrium is achieved very late in system's evolution (69,000 seconds). Negative fluxes are defined as being left to right.

an osmotic cell in an ideal and a non-ideal system. Both open-ended U-tube systems have the same geometry. A 1-cm thick membrane, having a cross-sectional area of 1 $cm^2$, separates solutions housed in the vertical arms which both have a circular, cross-sectional area of 0.008 $cm^2$. The initial conditions for the ideal system in Figure 3 and the non-ideal system in Figure 4 are also the same. The solution in the left arm (compartment I) contains 100 $cm^3$ of a 0.1 molal NaCl solution; the solution in the right arm (compartment II) holds 100 $cm^3$ of a 1.0 molal NaCl solution. Because the heights of these two solutions are initially equal, a small hydraulic pressure difference exists across the membrane due to slight density differences of the two solutions (Figures 3a and 4a).

To ascertain the way that both the ideal and non-ideal systems evolve with time, a computer program was written for the simultaneous solution of Eqs. (7) and (8) for the two fluxes at 1-sec increments, allowing for instantaneous mixing after each 1-sec flux interval. This iteration process resulted in a continuous recalculation of the $\sigma$, $\bar{c}_s$, $\Delta\Pi$, and $\Delta P$ variables. Fixed values were chosen for $L_p$ and $\omega$; the value chosen for $L_p$ was $10^{-9}$ $cm^3$/dyne·sec which translates to a conventional permeability coefficient for K of about $10^{-6}$ cm/sec. For the non-ideal system portrayed in Figure 4, $\sigma$ was assigned an initial value of 0.24 and $\omega$ was $10^{-11}$ mole/dyne·sec. The value assigned to $L_p$ is large when gauged from a geological perspective. Moreover, the value of $\omega$ is roughly five orders of magnitude higher than the maximum value of $\omega$ calculated by Eq. (13). These values were chosen to facilitate computer turnaround time which, in these examples, proved to be lengthy because of the 1-sec iteration intervals.

In response to the chemical potential difference of the water across the membrane, water from compartment I flows through the membrane to compartment II, resulting in a dilution of the 1 molal NaCl solution (Figures 3b and 4b). In the ideal membrane system, salt is retained in compartment I, resulting in an increase of the NaCl molality of this solution. The activity of water in compartment I decreases due to increased salt concentration; the water activity in compartment II increases due to dilution of the salt brought about by the osmotically driven water flux. The smaller differences between the activities values of water in the two solutions causes a decrease of potential osmotic pressure ($\Delta\Pi$) at that moment (Figure 3b). As osmotic flux continues from left-to-right, $J_v$ becomes less negative and $\Delta P$ becomes increasingly more positive as evidenced by the fluid levels in the U-tube arms. The net effect of the decreased $\Delta\Pi$ and increasing $\Delta P$ results in a continued diminution of the basic osmotic driving force, $\Delta\mu_w$. The ideal system continues to evolve until $\Delta\mu_w = 0$. At this point, the net solution flux across the membrane ($J_v$) is 0, resulting in the establishment of an osmotic equilibrium. At osmotic equilibrium in ideal membrane systems, the realized osmotically induced hydraulic pressure equals the theoretical osmotic pressure (Figure 3c).

A comparison of Figures 3 and 4 shows not only the difference in the magnitude of developed osmotic pressure, but also the manner in which osmotic equilibrium is approached. Inasmuch as the non-ideal membrane "leaks" salt, solute can diffuse through the membrane in a direction opposite to that of osmotic flow, $J_v$. Consequently, the potential osmotic pressures decrease

https://doi.org/10.1346/CCMN.1986.0340212 Published online by Cambridge University Press

very early in such a system's evolution, and the large hydrostatic head shown in Figure 3c for the ideal system cannot be realized for this non-ideal system. For a two-component aqueous system, the flux of solution, $J_v$, through the membrane at any time can be expressed by:

$$J_v = J_w \cdot \bar{V}_w + J_s \cdot \bar{V}_s, \quad (14)$$

where $J_w$ and $J_s$ are fluxes of water and salt, and $\bar{V}_w$ and $\bar{V}_s$ are the partial molar volumes of these components. There is no salt flux in an ideal system; hence, at all times, $-J_v = -J_w \cdot \bar{V}_w$ (Figures 3a and 3b). In contrast, salt flux is permitted in the non-ideal system. Although $J_s$ changes magnitude with time, its sign is positive so long as $\omega\Delta\Pi > \bar{c}_s(1 - \sigma)J_v$ (Eq. (8)). This condition should be typical of highly ideal membrane systems where $\sigma$ is close to unity. Here, the positive value of $J_s$ reflects the dominance of the diffusion of salt relative to the oppositely directed advection of the salt. In poorly permselective-membrane systems, characterized by very low values of $\sigma$, the salt flux may be dominated by advection such that both $J_v$ and $J_s$ are negative. At osmotic equilibrium for the non-ideal system, $J_v = 0$ because $-J_w \cdot \bar{V}_w = J_s \cdot \bar{V}_s$. Here, the maximum osmotically induced hydrostatic pressure ($\sigma\Delta\Pi$) is realized (Figure 4b). Because the clay membrane is permeable to salt, the quasi-equilibrium state of osmotic equilibrium depicted in Figure 4b is transient. Thereafter, the system "runs down" in an attempt to equalize the chemical potential differences of $H_2O$ and NaCl across the membrane (Figure 4c).

In Figure 5, the evolution of the ideal and non-ideal osmotic system is diagrammatically presented from the perspective of component fluxes. Substantial flux is generated early in the evolution of the ideal system, with the approach to osmotic equilibrium being gradual, in sharp contrast with the evolution of the non-ideal osmotic system. This evolution of a non-ideal osmotic system has three distinguishable events. First, osmotic equilibrium occurs and much quicker than in the ideal system. After osmotic equilibrium is established, the sign of $J_v$ changes from negative to positive, signifying a reversal of flow, with the net solution flux now being back toward compartment I. The second event is marked by $J_w \cdot \bar{V}_w = 0$, after which the positive fluxes of both water and salt combine to increase the rate at which the hydraulic head in the U-tubes is diminished. The third event is obtained when $J_v$ attains a maximum positive value; that is, when $dJ_v/dt = 0$. This point marks the beginning of de-acceleration of mass transport of solution back toward compartment I. The system then begins its long approach toward true equilibrium.

The dissipation rate of the osmotically induced hydrostatic pressure for the non-ideal system portrayed in Figures 4 and 5 is very gradual and is related to the magnitude of the generated osmotic pressure, which, in turn, is partially a function of solution parameters. The magnitude of the generated osmotic pressure, however, is also controlled by the membrane ideality. A value of $\sigma$ greater than the initially assigned quantity of 0.24 would have produced a greater realized osmotic pressure.

The build-up and dissipation of the osmotically induced hydrostatic pressure is also controlled by the values of all three phenomenological coefficients. System response is greatly controlled by the hydraulic permeability constant, $L_p$, of the membrane. The value of K for clays and shales is usually between $10^{-6}$ and $10^{-11}$ cm/sec (Freeze and Cherry, 1979). The $10^{-9}$ value chosen for $L_p$ corresponds to a K value of about $10^{-6}$ cm/sec. A value chosen to correspond to a less permeable membrane would have delayed the onset of osmotic equilibrium as well as prolonged the system's run-down toward true equilibrium. The role of $\omega$ is more subtle. Because $\omega$ is essentially a diffusive permeability coefficient, its value directly controls the rate at which the osmotic potential of the membrane cell is dissipated, i.e., the rate at which solute concentrations across the membrane becomes equalized. In the situation portrayed in Figures 4 and 5, the hydraulic permeability coefficient was sufficiently large to generate the initially high negative values for $J_v$. Thus, in the early stages of the evolution of this system, the back diffusional flux of salt was overwhelmed by $J_v$. Here, $\omega$ assumed an important role only in the dissipation of the osmotic pressure. Like $L_p$, a lower value assigned to $\omega$ would also have resulted in greatly extending the time between the establishment of osmotic and true equilibrium.

## HYPERFILTRATION

Hyperfiltration is sometimes invoked to explain solution chemistries in pore waters obtained from geologic formations (Bredehoeft *et al.*, 1963). Hyperfiltration is a membrane filtration process in which, upon application of a hydraulic gradient, solute concentration increases on the high pressure side of the membrane and more dilute solution issues from the downstream side (Fritz and Eady, 1985). Hyperfiltration occurs when the hydraulic pressure applied across the membrane, $\Delta P$, exceeds that of the realized osmotic pressure, $\sigma\Delta\Pi$. In terms of Eq. (7), hyperfiltration results when $\Delta P > \sigma\Delta\Pi$, i.e., when $J_v > 0$. Here, Eq. (8) shows that the resultant salt flux through the membrane is contributed by advection, $c_s(1 - \sigma)J_v$, as well as by diffusion, $\omega\Delta\Pi$. It should be emphasized that flow through a porous medium results in hyperfiltration only if the reflection coefficient of the porous medium $>0$.

Like osmosis, hyperfiltration can also be illustrated by a U-tube model. To prevent osmotic flux toward compartment II in Figure 3, a pressure of 41.22 atm would have to be applied to the solution in the right arm of the U-tube. An applied pressure greater than

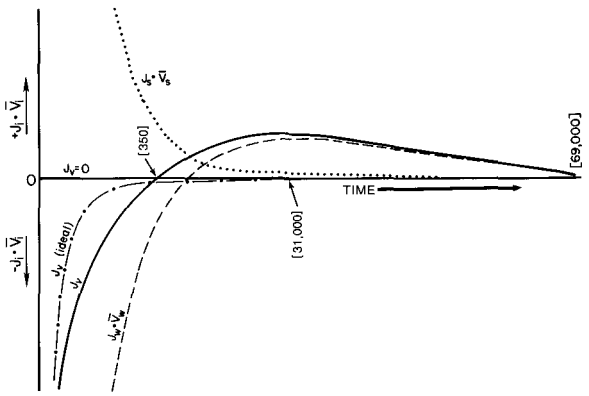


Figure 5. Diagrammatic sketch of evolution of osmosis in U-tube membrane systems depicted in Figures 3 and 4. Horizontal axis denotes zero net flux of solution. Positive fluxes occur above this line and represent fluxes toward compartment I in U-tube models. Particular events (in seconds) in evolution of these systems are given in brackets and correspond to events depicted in Figures 3 and 4.

41.22 atm would then force water into compartment I, raising the fluid level in the left arm of the U-tube. Hyperfiltration-induced flux ceases when the pressure applied to the more saline side of the membrane is counterbalanced by the effective osmotic pressure acting in the opposite direction. At this point $J_v = 0$ because $\Delta P = \sigma\Delta\Pi$ (Eq. (7)). For this reason, hyperfiltration is sometimes referred to as "reverse osmosis."

The ideality of membrane systems is gauged by the value of the reflection coefficient of the membrane. Because hyperfiltration is manifested when $J_v > 0$, the reflection coefficient is experimentally difficult to measure in such a dynamic system. For that reason, ideality of hyperfiltration systems is generally expressed as a measure of the salt rejected at the high pressure interface of the membrane. In their hyperfiltration experiments conducted on artificial sea water hydraulically forced through compacted clays, Kharaka and Berry (1973) reported filtration efficiencies of hyperfiltration for each ion in terms of a "filtration ratio." This value was defined as the ratio of an ion's concentration in the input solution to that in the effluent solution. Kharaka and Berry (1973) reported that the filtration ratios of most ions are greater than unity. In general, they found that high filtration ratios for ions were favored by low hydraulic gradients applied across highly compacted clays for dilute input solutions. Their findings were different in one respect from those reported by Kemper and Maasland (1964). The latter workers showed that salt sieving increased with increased pressure forcing solution across the clay.

## GEOLOGIC EXAMPLE OF OSMOSIS

In the subsurface, an osmotic cell is created when a difference of chemical potential of water exists across a membrane-functioning clay or shale. Special conditions must exist to generate osmotic flux and to prevent rapid dissipation of the resulting osmotically induced hydrostatic pressure. The membrane separating the two solutions must be of sufficient lateral continuity to prevent "short circuiting" of flow around the unit. The likelihood of detecting osmotically induced hydrostatic pressure in the subsurface will probably be greatest if the reservoir receiving the osmotic flux is bounded peripherally by extremely impermeable materials. This situation would tend to preserve the generated osmotic pressure for longer times than if both sides of the membrane had communication with an active ground-water flow system.

Such a situation was described by Marine and Fritz (1981) who investigated the hydrology of a buried Triassic basin overlain by coastal plain sediments of Cretaceous age. The buried Triassic basin is a graben structure set in gneiss and schist country rock (Figure 6). Sediment within the Triassic basin consists of intercalated lenses of fine sand and clay. The clay is mainly illite, and the average porosity of the sediments is 3.5% (Marine, 1974). Four wells penetrate the basin (Figure 6); all wells were cased to below the Triassic-Cretaceous contact so that the water sampled from these wells was representative of pore water within the Triassic sediments. The two wells penetrating deep into the basin yielded saline water. The total dissolved solids of water from well DRB-10 was 11,900 ppm; that for well DRB-11 was 18,500 ppm (Marine and Fritz, 1981). Both wells were capped because their hydrostatic heads were above the local land surface and well above the local water table developed in the Cretaceous sediments (58 m above sea level).

Marine and Fritz (1981) concluded that osmosis was the most likely cause of these anomalous hydrostatic heads. In this situation, fresh water (TDS ~ 40 ppm) from the overlying coastal plain sediments was driven by osmosis into the saline pore water contained within the Triassic sediments. The Triassic sediments acted as a composite membrane, in that individual clay lenses acted as discrete membranes separating saline solution housed within adjacent arenaceous pods. The activities of water in solutions sampled from wells DRB-10 and DRB-11 were measured against the activity of water in the overlying coastal plain sediments. The calculated theoretical osmotic pressures for solutions in these two wells was then calculated by Eq. (3) and compared to the observed hydrostatic heads. The more saline water of well DRB-11 was calculated to have a theoretical osmotic pressure of 178 m of head above sea level, compared with the observed head of 192 m. The less saline water of well DRB-10 gave a calculated $\Delta\Pi$ of 136 m of head above sea level as opposed to the observed level of 140 m. In these calculations, Marine and Fritz (1981) assumed that the illitic membrane of the Triassic basin was ideal. Judged from the viewpoint

https://doi.org/10.1346/CCMN.1986.0340212 Published online by Cambridge University Press

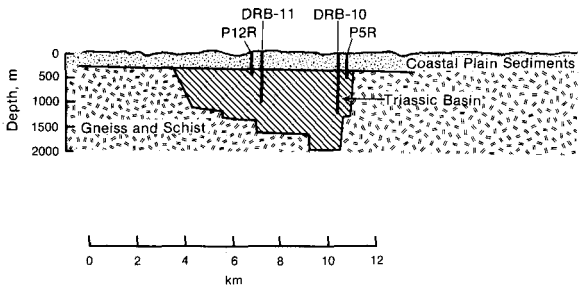


Figure 6. Cross section of buried Dunbarton Triassic basin near Aiken, South Carolina. Deep wells penetrating saline heart of basin are osmotically pressurized. Two wells barely penetrating basin show little anomalous head character and yield water low in total dissolved solids.

of the factors controlling the ideality of clay membranes, this assumption seems reasonable. If the low-porosity illites in the clay lenses of the Triassic sediments have a CEC of 20 meq/100 g, the calculated $\sigma$ values for this membrane in contact with waters of wells DRB-10 and DRB-11 are 0.97 and 0.95, respectively.

The other two wells which barely penetrate the basin exhibited no anomalously high fluid pressures. Well P5R had an observed hydraulic head 5 m above the local surface (Marine and Fritz, 1981). No chemical data exist for this well, but well P12R had a total dissolved solids content of only 800 ppm. Thus, the two deep wells (DRB-10 and DRB-11) appear to be within the saline heart of the basin. The outer margins of the presumed, originally saline basin have diffused their salt away toward the fresh water housed within the overlying Coastal Plain sediments. The overall osmotic driving force toward the deeper, more saline part of the basin provides a cause for fluid containment apart from the low permeability of the Triassic sediments. If the upward-acting hydraulic gradient was balanced by the downward-directed osmotic gradient, no net force existed to cause unidirectional fluid movement toward the overlying fresh aquifer. Here, $J_v$ was probably very small, and the eventual demise of the entire osmotic cell of the Triassic basin was controlled by the rate at which salt diffused out of the basin. Because an osmotic cell is active so long as a difference of salt concentration exists across the membrane, this osmotic cell probably has been operating since the establishment of fresh water within the pores of the overlying Cretaceous sediments.

## SUMMARY

The evolution of an osmotic system is controlled by the values of the phenomenological coefficients as well as by the initial osmotic driving force acting across the membrane. The hydraulic permeability constant, $L_p$, is a measure of the system's sluggishness of response in terms of transporting solution and solute through the membrane structure. In general, low values of $L_p$ correspond to highly compacted membranes, resulting in enhanced membrane ideality. Highly ideal membranes have values of $\sigma$ close to unity and $\omega$ values approaching 0. Such systems should exhibit initially high osmotic fluxes resulting in a gradual approach toward osmotic equilibrium. If the osmotically induced hydrostatic pressure in this type of system is substantial, the back diffusion of salt causing the eventual demise of the system should be extremely slow. In contrast, poorly ideal membrane systems should establish osmotic equilibrium early in their evolution relative to the time at which true equilibrium is finally achieved. Because of the leaky nature of this type of membrane system, salt is transported across the membrane by advection and diffusion which has the effect of rapidly equalizing the salt distribution across the membrane and results in a continuous and rapid diminishment of the osmotic potential of the cell.

Sediments within the Dunbarton Triassic basin acted as a composite membrane and as the saline reservoir. A unique osmotic cell was created by the juxtaposition of the fresh water in the overlying Coastal Plain sediments against the saline pore water housed within the pores of the membrane-functioning sediments of the Triassic basin. The osmotic gradient drove water into the saline reservoir surrounded peripherally by impermeable basement rock. Because the Triassic sediments were nearly ideal membranes, the resultant osmotically induced hydrostatic pressure was substantial for wells penetrating the saline interior of the membrane complex. Osmotic cells like these should dissipate their solutes from the interior toward the outer margins in contact with fresh water. Thus, wells barely penetrating the basin showed no substantial anomalous heads and yielded waters that were much less saline than that obtained from the basin's interior.

## ACKNOWLEDGMENTS

Acknowledgment is made to the donors of the Petroleum Research Fund, administered by the American Chemical Society, for support of this research (14765-AC2).

## REFERENCES

Bredehoeft, J. D., Blyth, C. R., White, W. A., and Maxey, G. B. (1963) Possible mechanisms for concentration of brines in subsurface formations: *Amer. Assoc. Pet. Geol. Bull.* **47**, 257–269.

Freeze, R. A. and Cherry, J. A. (1979) *Groundwater:* Prentice-Hall, Englewood Cliffs, New Jersey, 604 pp.

Fritz, S. J. and Eady, C. D. (1985) Hyperfiltration-induced precipitation of calcite: *Geochim. Cosmochim. Acta* **49**, 761–768.

Fritz, S. J. and Marine, I. W. (1983) Experimental support for a predictive osmotic model of clay membranes: *Geochim. Cosmochim. Acta* **47**, 1515–1522.

Gregor, H. P. and Gregor, C. D. (1978) Synthetic membrane technology: *Sci. Amer.* **239,** 112–128.

Grim, R. E. (1968) *Clay Mineralogy:* McGraw-Hill, New York, 596 pp.

Hanshaw, B. B. (1962) Membrane properties of compacted clays: Ph.D. dissertation, Harvard University, Cambridge, Massachusetts, 113 pp.

Hanshaw, B. B. (1964) Cation-exchange constants for clays from electrochemical measurements: *Clays and Clay Minerals, Proc. Natl. Conf., Atlanta, Georgia, 1963,* W. F. Bradley, ed., Pergamon Press, New York, 397–421.

Hanshaw, B. B. and Zen, E. (1965) Osmotic equilibrium and overthrust faulting: *Geol. Soc. Amer. Bull.* **76,** 1379–1387.

Harned, H. S. and Owen, B. B. (1958) *The Physical Chemistry of Solutions:* Reinhold, New York, 803 pp.

Hudec, P. P. (1980) Hypersaline brine and clay liner interaction: in *Proc. 3rd Int. Symp. Water-Rock Interaction, Edmonton, Alberta, 1980,* Alberta Research Council, Edmonton, Alberta, 153–154.

Katchalsky, A. and Curran, P. F. (1965) *Non-Equilibrium Thermodynamics in Biophysics:* Harvard University Press, Cambridge, Massachusetts, 248 pp.

Kedem, O. and Katchalsky, A. (1962) Permeability of composite membranes. I: Electric current, volume flows and flow of solute through membranes: *Trans. Faraday Soc.* **59,** 1918–1930.

Kemper, W. D. and Maasland, D. E. L. (1964) Reduction of salt content of solution on passing through thin films adjacent to charged surfaces: *Soil Sci. Soc. Amer. Proc.* **28,** 318–323.

Kemper, W. D. and Rollins, J. B. (1966) Osmotic efficiency coefficients across compacted clays: *Soil Sci. Soc. Amer. Proc.* **30,** 529–534.

Kharaka, Y. K. and Berry, F. A. (1973) Simultaneous flow of water and solutes through geologic membranes, I. Experimental investigation: *Geochim. Cosmochim. Acta* **37,** 2577–2603.

Kharaka, Y. K. and Smalley, W. C. (1976) Flow of water and solutes through compacted clays: *Amer. Assoc. Pet. Geol. Bull.* **60,** 973–980.

Marine, I. W. (1974) Geohydrology of a buried Triassic basin at Savannah River plant, South Carolina: *Amer. Assoc. Pet. Geol. Bull.* **58,** 1825–1837.

Marine, I. W. and Fritz, S. J. (1981) Osmotic model to explain anomalous hydraulic heads: *Water Resources Res.* **17,** 73–82.

McKelvey, J. G. and Milne, I. H. (1962) The flow of salt solutions through compacted clays: in *Clays and Clay Minerals, Proc. 9th Natl. Conf., West Lafayette, Indiana, 1960,* Ada Swineford, ed., Pergamon Press, New York, 248–259.

Miller, D. G. (1966) Applications of irreversible thermodynamics to electrolyte solutions. I. Determination of ionic transport coefficients $l_{ij}$ for isothermal vector transport processes in binary electrolyte system: *J. Phys. Chem.* **70,** 2639–2659.

Olsen, H. W. (1969) Simultaneous fluxes of liquid and charge in saturated kaolinite: *Soil Sci. Soc. Amer. Proc.* **33,** 338–344.

Robinson, R. A. and Stokes, R. H. (1959) *Electrolyte Solutions:* Academic Press, New York, 512 pp.

Srivastava, R. C. and Avasthi, P. K. (1975) Non-equilibrium thermodynamics of thermo-osmosis of water through kaolinite: *J. Hydrology* **24,** 111–120.

Staverman, A. J. (1952) Non-equilibrium thermodynamics of membrane processes: *Trans. Faraday Soc.* **48,** 176–185.

Stumm, W. and Morgan, J. (1970) *Aquatic Chemistry:* Wiley-Interscience, New York, 583 pp.

Tuwiner, S. B. (1962) *Diffusion and Membrane Technology:* Reinhold, New York, 421 pp.

White, D. E. (1965) Saline waters of sedimentary rocks: in *Fluids in Subsurface Environments,* A. Young and J. Galley, eds., American Association of Petroleum Geologists, Tulsa, Oklahoma, 414 pp.

Young, A. and Low, P. F. (1965) Osmosis in argillaceous rocks: *Amer. Assoc. Pet. Geol. Bull.* **49,** 1004–1008.

*(Received 29 January 1985; accepted 7 June 1985; Ms. 1447)*